Jurnal Teknologi

Full Paper

MOTION CHARACTERIZATION OF A SWITCHED RELUCTANCE ACTUATOR – A SIGNAL DRIVEN APPROACH

Mariam Md Ghazaly[a,b*], Izzati Yusri[a,b], Muhammad Shadiq Lagani[a,b]

[a]Center for Robotic and Industrial Automation (CeRIA), Universiti Teknikal Malaysia Melaka, Hang Tuah Jaya, 76100 Durian Tunggal, Melaka, Malaysia
[b]Fakulti Kejuruteraan Elektrik, Universiti Teknikal Malaysia Melaka, Hang Tuah Jaya, 76100 Durian Tunggal, Melaka, Malaysia

Article history
Received
30 April 2021
Received in revised form
1 August 2021
Accepted
4 August 2021
Published online
20 August 2021

*Corresponding author
mariam@utem.edu.my

Graphical abstract

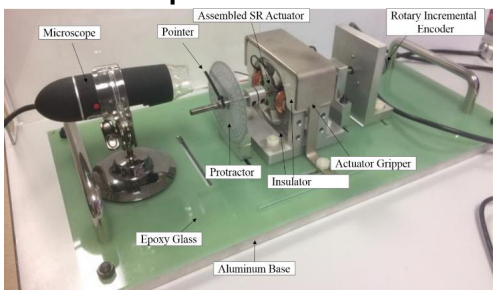

Abstract

In this paper, the researchers have described the development, design and characterization of a Switched Reluctance (SR) actuator, with a rotary motion, having a single-excitation activity. This SR actuator design consisted of a stator and rotor core and was based on the simplest SR actuator model design, with a Stator-to-Rotor pole ratio (S: R) of 6:4. In this design, the winding was coiled at Phase A, which enabled the single step motion characterization based on a single excitation. This SR actuator prototype showed a compact size, with a 36 mm stack length and a 60 mm outer diameter. This feature allowed small machine applications like the precision robotic machining, but required a low production cost, as it lacked a permanent magnet. On the other hand, the SR actuator consisted of highly non-linear characteristics and showed uncontrolled motion behavior. While achieving a very precise motion, it is important to suppress the non-linear characteristics of an actuator. Hence, the researchers designed the linearizer unit based on its characterization at Position 0°, which was related to the excitation current and the rotary angles for the various initial rotor positions. This initial position was chosen as it reflected the characteristics which indicated the self-starting characteristics. Thereafter, the researchers experimentally investigated the appropriate driving signal for this SR actuator as the normal step input signal showed a lower precision motion because of the discharging effect-related issues. Based on these results, the researchers selected a pulse input signal of 20Hz and 1:4 duty ratio as the appropriate driving signal, which could improve the motion characteristics.

Keywords: Switched reluctance actuator, motion characterization, driving signal

1.0 INTRODUCTION

Many researchers have used the precision motion system in different applications like the semiconductor manufacturing processes, pick-and-place robotic systems or small machine applications, i.e. micro-gripper [1, 2]. Generally, these systems consist of an appropriate actuator. Recent studies highlighted 4 main characteristics of an actuator: (i) Low cost of construction; (ii) A basic geometrical design; (iii) A high value of the generated torque and; (iv) A higher precision motion [3–6]. Currently, many actuators display a precision motion [7–12]. The piezoelectric and the electrostatic actuators were seen to be

common linear motion actuators, which displayed a shorter working range [13]. On the other hand, the pneumatic and the electromagnetic actuators could display a large working range. In the past few years, the developed electromagnetic actuator displayed rotary motion behavior.

In the past, researchers developed a rotary, high precision, electromagnetic actuator as the Stepper Motor type [14–17]. This actuator operated the micro-stepping size dependents on the pole's slot and showed a maximal 5% noncumulative position error for every step. However, this system performance was only possible if a permanent magnet was used in the actuator design for each step input.

The Switched Reluctance (SR) actuator is a different electromagnetic actuator, which has become more popular in the past few years, due to its lower construction cost and simple structure [18, 19]. Furthermore, the SR actuator is rugged, shows a faster response and requires a low maintenance due to its simple design structure [20]. The SR actuator can drive in the incremental or continuous operations [21]. These operations are based on all motion characteristics, dependent on an excitation current applied. The general SR actuator was made of 2 material types, i.e., the rotor/ stator had a soft-iron core, and a copper wire [3]. This soft-iron core used the winding turn's current excitation and offered the magnetic flux a low reluctance pathway [22]. The rotor moves in a manner which decreases the reluctance (i.e., aligned positioning) and generated the torque for the rotary motion. Owing to its simple structure and operational principle, the SR actuator has garnered a lot of popularity after the development of Electric Vehicles (EV), since it can generate a high torque and display a very speedy performance [23–26].

On the other hand, the SR actuators display very non-linear characteristics and uncontrolled motion behavior. Some recent studies have acquired a higher precision motion using characterization techniques for suppressing the non-linear characteristics like the hysteresis effects and friction [9]. While designing the SR actuators, many researchers focused on the application of a constant drive for operating the motor system and the Switched Reluctance Motor (SRM). However, the precision motion performance was a secondary issue owing to the non-linearity-related problems. According to [27], if the switching SRM profiles were controlled properly, they would help the actuators display a better motion precision at higher speeds.

The major difference between the SRM and the SR actuators was their rotatory behavior during the continuous or the fixed step during all operations, as presented in Table 1. In the SR actuator, the applied controller was targeted toward the positioning requirement. In their study, [27] observed that an SR actuator behaved as a servo if it was controlled properly and could achieve a 90% efficiency. Though the SR actuator needs the help of an expensive position sensor for detecting the immediate rotor positions, its lower construction cost and lesser maintenance can overcome all its limitations. The SR and the SRM actuators displayed similar characteristics, except for their controlled strategy and end results. This further led to the application of the SRM as the precision motion actuator or an SR actuator. Many studies adopted the SR actuator as a high-precision motion rotor [9, 28, 29], which was further used for developing a linear actuator rather than a rotary model. These actuators have become very popular due to their high precision motion and low cost, however, their non-linear properties have made them very difficult to control.

Table 1 A comparison of the SRM and the SR actuator characteristics

Characteristics	Switched Reluctance Motor (SRM)	Switched Reluctance (SR) actuator
Coil Excitation	Multi-phase	Single-coil
Motor Drive	Continuous/ Incremental	Incremental
Controlled Variable	Torque	Position
Motion Characteristic	Continuous	Fixed angular step
Geometrical Construction	Similar design	
Characteristic Model	Nonlinear	

In the past, many researchers used the linearization method for eliminating the nonlinear characteristics of the various actuators [6, 9, 30–32]. Their main objective was to suppress and eliminate the non-linear characteristics of hysteresis and uncontrolled magnetic flux distribution in the electromagnetic systems, which enabled the implementation of the actuators in combination with the traditional PID controllers. This linearization technique offered a predetermined characteristic data for the mover position, thrust force and the excitation current. Though the controller was seen to be less robust, the application of the linearization method in the model was very reliable. Furthermore, owing to the variation in the performances due to different excitation current signals, the researchers must configure the driving signals more accurately, for improving the precision motion system with the help of the linearization method. If the linearization method is implemented in the SR actuators, the low cost and the control strategy could decrease the overall expenses.

In this study, the researchers developed and characterized the rotary SR design, described earlier [33, 34], for acquiring the linearizer unit for a specific design along with its related driving signal configurations. For this purpose, they adopted a single-excitation technique and developed a linearizer unit for the one-step motion. They also presented an appropriate driving signal at the self-starting position for improving the rotary motion performance compared to a normal step input signal. Section 2 presented the structure and the working principle of an SR actuator; while Section 3 presents the

experimental setup. Section 4 discusses the open-loop characteristics of the SR actuator, which were used for determining the linearizer units based on the rotational motion characteristics. Section 5 presents the configuration of the appropriate driving signals which could be used for enhancing the dynamic motion performance compared to the normal driving signals. Lastly, Section 6 presents all the conclusions.

2.0 THE STRUCTURE AND THE WORKING PRINCIPLE OF AN SR ACTUATOR

2.1 SR Actuator Structure

The SR actuator consisted of 3 distinct features; (i) Absence of any permanent magnet; (ii) The stator and the rotor core showed a basic geometrical structure, and (iii) A compact size with a low excitation current. The basic SR actuator structure is described in Figure 1, based on all the parameters described in Table 2. As shown Figure 1, the model consists of a stator and a rotor core. Also, the 6 stator poles consisted of some wound copper wires, which were color-coded, as described in Table 3, for enabling the 3-phase actuation process during the actual operation. The copper wires with 5 mm thickness were used since it could withstand the maximal excitation current that could be applied to an SR actuator, i.e. 2A.

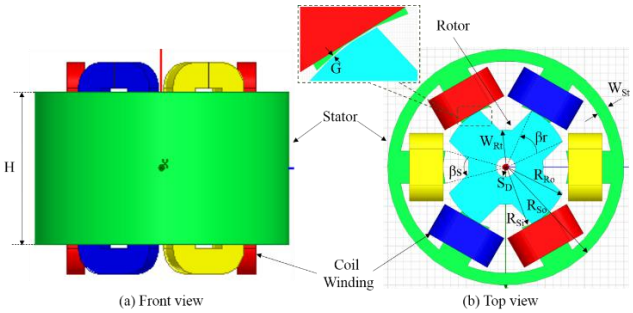

Figure 1 The basic structure of an SR actuator

Table 2 The configuration of the various SR actuator parameters

Parameters	Value
Stator outer radius, RSo	30 mm
Stator inner radius, Rsi	15.9 mm
Rotor outer radius, Rro	15.8 mm
Air gap thickness, g	0.2 mm
Winding number, N	60 Turns
Stack length, H	36 mm
Stator arc angle, βs	29°
Rotor arc angle, βr	40°
Rotor thickness, WRt	5 mm
Stator thickness, WSt	3 mm
Shaft hole diameter, SD	5 mm
Stator weight	325gm
Rotor weight	150g

Table 3 Labelling of the 3-phase SR actuator system parameters

Parameter	Label
Phase A	
Phase B	
Phase C	
Stator	
Rotor	

The stator and the rotor core of the SR actuator were made of the medium carbon steel material, i.e., S45C, with a B-H curve, as described in Figure 2. The researchers did not use laminated silicon steel in this study. This further decreased the SR actuator construction costs. Additionally, the use of the carbon steel material increased the tensile strength of the actuator, which prevented its deformation and made them more durable under harsh environmental conditions. As this material did not require any lamination, the eddy current effect was reduced by lowering the applied current frequency, such that the maximal applied frequency was 20Hz. This minimized the heat generated due to the eddy currents effects in the SR actuator.

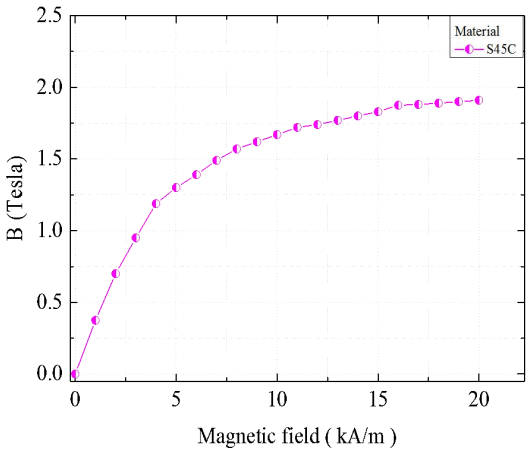

Figure 2 A B-H curve of the medium carbon steel material, S45C

2.2 Working Principle

Figure 3(a) describes the working principle of the single-excitation Phase A of the SR actuator, placed at an unaligned position, whereas the other phases, like the Phase B and C, were set at 0A current. As described in Figure 3(a), the flux, developed from the excited Phase A1, could move the rotor core towards the Phase A2 pole, because of the minimal reluctance presented by this core. As the rotor position was unaligned, the rotor could rotate in a Counter-Clockwise (CCW) direction, which aligned the rotor and stator poles shown in Figure 3(b). This rotor remained in the assigned position, only if no external

force was exerted and the excitation current was not cut-off. On the other hand, if a reverse rotation (Clockwise, CW) was needed, the C1 and C2 poles would be excited. The CCW and CW directions were based on the immediate rotor position, hence, the rotational and torque characteristics, in all positions, helped to control the actuator motion. The working principle was based on the single-excitation SR actuator, as described earlier [35].

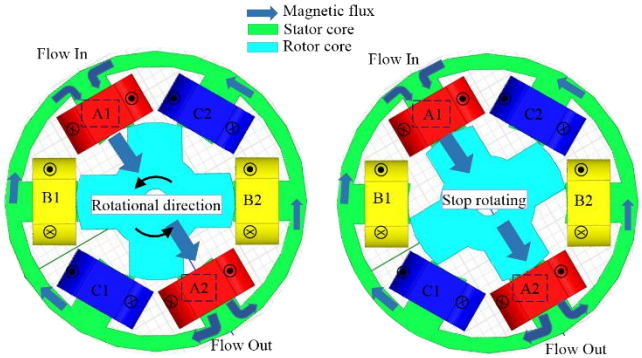

(a) Unaligned (b) Aligned

Figure 3 A top view of the single-excitation, magnetic A1-A2 circuit [35]

3.0 PROTOTYPING SR ACTUATOR

The stator and the rotor core of the SR actuator were made of the medium carbon steel material, i.e., S45C, as described in Figure 4(a). For preventing the direct contact of the stator with copper wire, the inner stator surface was insulated with the help of a 0.1 mm thick Nomex 410 thermal sheet insulation paper. Phase A was coiled with a 0.5 mm thick copper wire (60 turns/coil), which enabled the single-excitation characterization. Presence of the mutual induction in the adjacent coils would increase the saturation effect, which highlighted their non-linear characteristics [36] and disrupt the linearization of the single-excitation properties. The diameter of this copper wire was based on the maximal capacity of the permissible current, i.e., 3A for a 0.5 mm thickness. For the similar phasic poles, the copper coil is wound in the similar direction, i.e., CW, as described in Figure 4(b), for ensuring the magnetic flux, shown in Figure 3, thereby completing the magnetic circuit. The coils were connected in series, wherein the input current would flow through the Coil winding A1 and flow out through the Coil Winding A2, as shown in Figure 5.

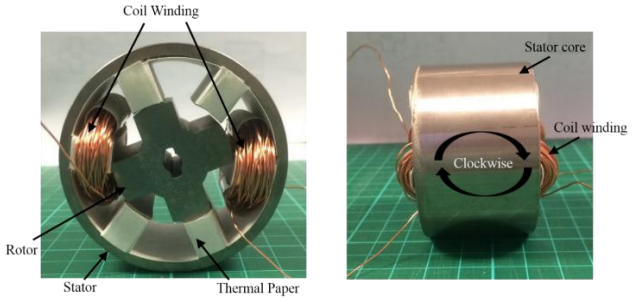

Top view (b) Side view

Figure 4 Assembly of the SR actuator model including the insulation and coil winding

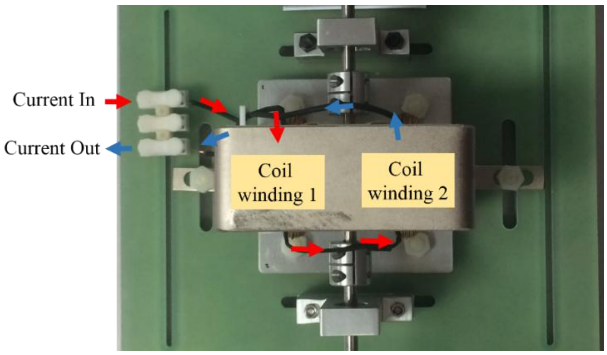

Figure 5 The direction of the flow of the current through the coil winding

Figure 6 presents the general experimental setup for characterizing the single-excitation properties. Here, the SR actuator was assembled without any casing, which helped in setting and monitoring its mechanical motion. The rotor was fixed in the stator, with the help of higher precision ball bearings, which resulted in a frictionless rotor with a 0.2 mm air gap. Furthermore, the stator was fixed with the help of a stator holder to an insulated based. 2 couplings were used for connecting the ball bearings and the rotor shaft. This helped in preventing the use of a long rotor shaft, which caused a bending of the shaft at its center, because of its rotor weight, which further led to an uneven rotation. All the holder and base materials were made of aluminium.

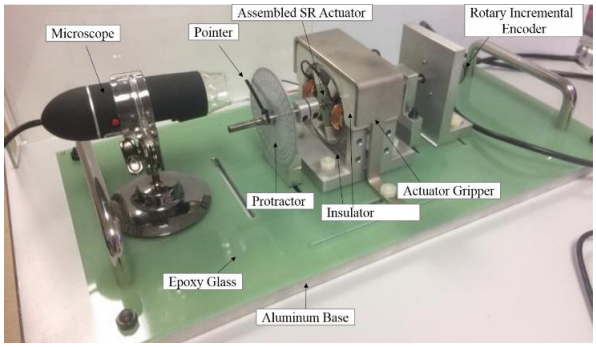

Figure 6 Assembly of the complete experimental setup

In this research, the Scancon Incremental Rotary Encoder was implemented for measuring the output rotary angle at the end of an actuator shaft. As the rotor position is very important, the microscope can ensure that the rotor was present at its assigned initial position for every repetition as the rotor was manually rotated. The rotor position could be adjusted using a protractor or indicator, as described in Figure 6. Owing to the limitations of the experimental set-up, the torque value could be estimated using the encoder-based rotary motion. Some studies [37] calculated the generated torque (Nm) value, using the product of the acceleration (rad/s2) and the rotor's moment of inertia (kg m2) if the rotor was operational. Therefore, in this study, the researchers have used the technique of second differentiation with the help of the MATLAB Simulink software, for profiling the torque values of the SR actuator.

4.0 MOTION CHARACTERIZATION

The researchers used the linearization method for characterizing the various rotor positions using the same current excitation signal, which is a step input signal with differing magnitudes, ranging from 0A to 2A. They nalysed the different initial rotor positions based on the correlation of the changes seen in the generated torque, using Equation (1) [38]:

$$\tau = \frac{1}{2} i^2 \frac{dL(\theta, i)}{d\theta} \quad (1)$$

wherein I = excitation current, θ = rotor position, while L = varied inductance based on the overlap between the stator and the rotor pole. The proper torque profile could be generated from these characterizations, which indicates all torque magnitudes with a differing polarity (that highlights the tendency of the rotational direction). Furthermore, the researchers configured the rotational motion with regards to their different positions, and thereafter, the selected position could be used for designing the linearizer units.

4.1 Torque Characterization

Figure 7 highlights the relation between the different rotor position, ranging from 0° to 80°, at a 10° interval, and the excitation current, from 0A to 2A, at a 0.5A interval. The symbol indicated the estimated values, while the line represented the approximate curve, which was estimated from this data. The 2 parameters were simultaneously varied in all experiments. The experiment was performed 20 times, for improving the data reliability.

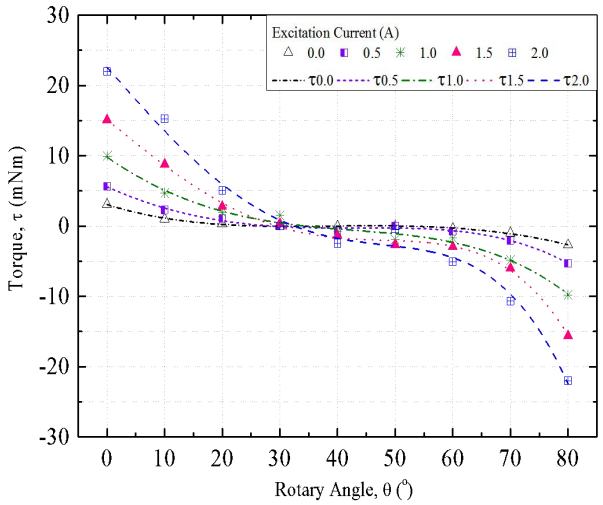

Figure 7 Comparison of the generated torque value after varying the initial rotor positions

As only the Phase A was excited, the torque generated would display an identical magnitude, but different polarities or positions. This polarity indicated the tendency of the rotational direction, wherein the positive or negative values represented the CCW or the CW direction, respectively. Figure 7 shows that the maximal torque magnitude was noted in the 0° and 80° positions, for all the excitation current amplitudes. Though it was an unaligned position, it still required sufficient energy for initiating the rotation and producing acceleration, which was further used for generating the torque. However, this was not noted for rotor positions between 30° and 50°, which were considered to be a stable equilibrium position, based on their aligned poles, as seen in Figure 8. Hence, they showed a low rotational tendency, so that their magnetic flux flowed effortlessly, owing to a smaller air gap and a lower reluctance pathway.

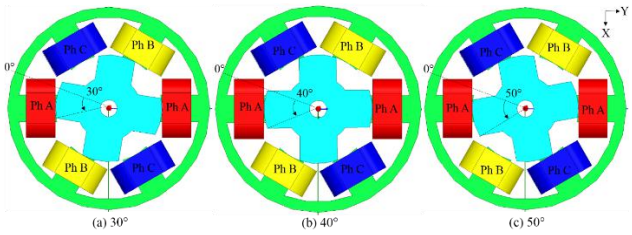

Figure 8 The initial rotor positions for the aligned stator and rotor poles

Generally, the unaligned position (i.e., 0° and 80°) showed a few rotational tendencies, due to a higher reluctance pathway. On the other hand, the data showed an opposing effect. This property was related to the discharging effect as the SR actuator was used 20 times for every test at a 10 s interval for decreasing the accumulated magnetic flux inside the core.

Hence, for evaluating the discharging performance of the SR actuator, the researchers conducted several SR actuator-based experiments using different test period intervals. A maximal excitation current of 2A was applied at the 0° rotor position, while the surrounding temperature was controlled, wherein the temperature difference was <1°C. Table 4 presents the flux discharge percentage with regards to the remaining time period. The medium carbon steel material, grade S45C, showed a low discharge rate. Within a 7-day rest time period, this SR actuator showed a 6.81% decrease in the accumulated magnetic flux. On the other hand, for a 15 min rest time period, the SR actuator displayed a negative value, which showed that the SR actuator did not get discharged owing to a shorter rest time period. In many real applications, a smaller discharge rate helps in maintaining the actuator performance for many continuous operations, as no extra time is needed for reaching the maximal generated torque, as the SR actuator was operational within the saturation area. However, it could exceed all saturation effects if it was supplied with the current. Hence, an appropriate driving signal was needed for a discharge for improving the torque and all motion characteristics during its operation.

Table 4 The SR actuator magnetic flux discharge depending on varying rest time periods

Rest Time Period	Temperature (°C)	Torque (mNm)	Magnetic flux discharge (%)
15 minutes	21.5	22.050	-0.38
30 minutes	21.5	21.900	0.31
1Hour	21.2	21.690	1.26
1 Day	21.3	21.510	2.08
1 Week	22.3	20.470	6.81

For designing a more compact actuator model, the researchers noted that the generated torque performance was sufficient for many applications, like biomedical tools, which required higher precision motion control. This was similar to the common hybrid stepper motor, which showed smaller actuator properties but required an expensive permanent magnet [39]. A high torque was not necessary for many practical applications, as it led to a higher overshoot and affected the electronic components during the motion. In one study, [29] investigated the Variable Reluctance (VR), two-finger gripper that applied a low torque, i.e., a maximal of 50 mNm, for generating the required 600 nM force that could satisfy all grasping conditions.

4.2 Rotational Characteristics

For linearizing the rotational motion of the SR actuator, the researchers measured the characteristics of the various initial rotor positions using a single-step response. In the case of different step input signal magnitude values, the rotational motion constantly changed for every repetition test, indicating the non-linear motion behavior. Figure 9 presents the compiled rotary motion which settles the response position with regards to the excitation current. The researchers noted that the maximal torque generated at 0° and 80° positions, in Figure 7, led to the maximal rotary angle for these positions, however, they showed opposite rotational directions. This was attributed to the fact that the initial position was completely unaligned, and therefore required a large rotary angle to attain the aligned position. Since the rotor was placed in an aligned position, between 30° and 50°, the resulting rotary angle was very small or even motionless. Hence, the rotor would move with a smaller generated torque magnitude, exerted by the rotor, since it would be in a stable equilibrium, owing to the larger overlapping angle value between the two poles.

For identifying the motion performance, the researchers analysed a single response. They investigated the parameters like the settling time (Ts), percentage overshoot (%OS), standard deviation (σ) and the position error as response parameters at the initial 0° position (fully unaligned), because of the important self-starting conditions, while applying the intermediate current excitation magnitude of 1A at Phase A. As the SR actuator rotated in one step for every excitation, it helped in conducting the observation performances, though all experimental work had to be conducted in an open-loop. Figure 10 and Table 5 describe the single response and performance of the rotational motion, respectively.

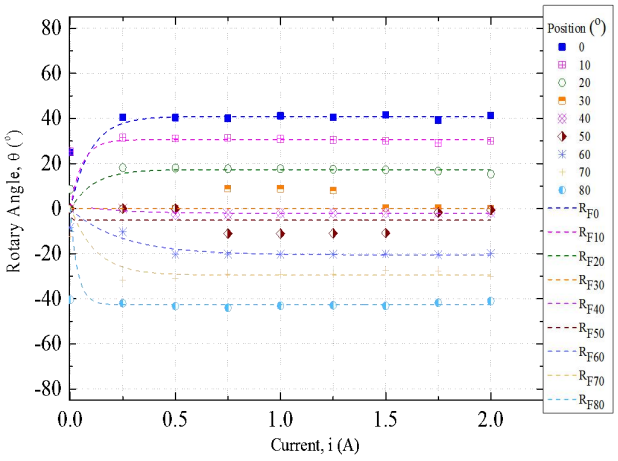

Figure 9 Rotational characteristics noted after varying the initial positions and the excitation current

The characteristics indicated that the step input signal displayed a higher % OS and settling time. This could be due to a sudden surge of the accumulated magnetic flux at a low discharge rate, as mentioned in Section 4.1. This could result in the overshoot being overwhelmed with the constant experimental work

being carried out. Owing to an uncontrolled magnetic flux, the repeatable responses showed a high standard deviation, which further decreased the reliability of a high precision motion. Furthermore, the position error was relatively high, in comparison to the reference position, which was measured to determine if it was completely aligned with the excited Phase A at the stator and the rotor poles. This highlighted the inappropriateness of using the step input signal, which could be improved further using alternative driving signal configurations.

After characterization, the researcher selected the settling rotary angle characteristics at the initial 0° position, shown in Figure 9, as the linearizer unit, described in Figure 11. This was defined as the critical self-starting condition, owing to the completely unaligned and higher reluctance. In this study, the linearizer unit was designed for cancelling the non-linear characteristics of electromagnetism in an SR actuator, and the appropriate excitation current was predetermined for acquiring the final position. Hence, the x and y-axis represented the rotary angles and the excitation current, respectively. All the symbols in Figure 11 present the measured values, whereas the solid line presents an approximate linearizer unit. Eq. 2 presents the output function of a linearizer.

$$R = -0.001\,9 + ln\frac{(i - 40.89)}{-41.686}(0.095) \quad (2)$$

wherein; R describes the rotary angle; while the excitation current was presented as i.

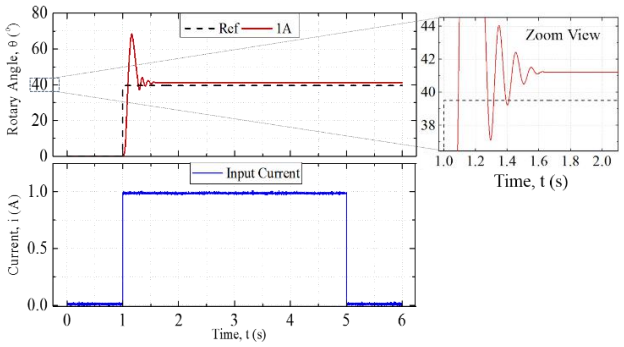

Figure 10 A single rotational response of 1A current at the initial 0° position

Table 5 The output response characteristics of 1A current at the initial 0°

Characteristic	Magnitudes
Percentage Overshoot, %OS (°)	65.98
Settling time, Ts (s)	1.412
Standard Deviation, σ (°)	1.000
Position error (°)	1.725

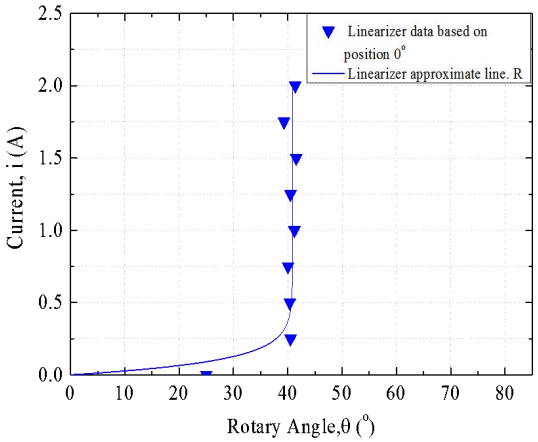

Figure 11 The rotary motion characteristics at the initial 0° position

For fulfilling all the rotary motion characteristics, the researchers added the rotary angle of a negative step input signal as shown in Figure 12. The SR actuator was unaffected by all changes occurring in the polarity of the excitation current, while the negative amplitude led to the same direction. Hence, the approximate line of the linearizer was mirrored with the x-axis.

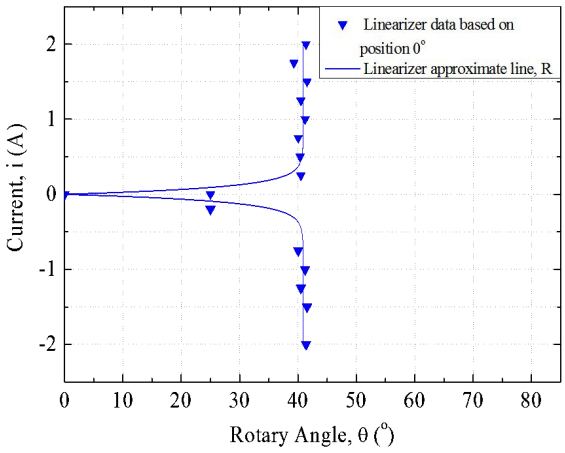

Figure 12 The linearizer unit depending on the motion characteristics of an SR actuator with regards to the step input signal applied

This linearizer unit was applied to a classical PID controller as shown in Figure 13. The researchers stipulated that the maximal excited current should satisfy all conditions, which were below the magnitude of i = ±2A. If a higher current was applied, which exceeded this limitation; it could alter the motion characteristics. Therefore, for differing SR actuator designs, the new actuators would need a different linearizer unit. In this study, the researchers have proposed a novel method for linearizing any type of rotary electromagnetic actuator. They also stated that

for changing any of the geometrical design parameters, like stator outer diameter, DSO, or stack length, H, a similar linearizing method could be used.

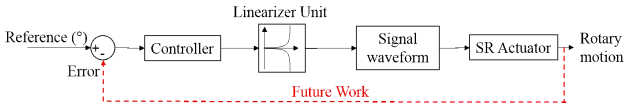

Figure 13 Application of the linearizer unit in different control systems

5.0 EFFECTS OF DRIVING SR ACTUATOR SIGNAL TO MOTION CHARATERISTICS

As described in Section 4, the applied step input signal showed a higher percentage of the accumulative magnetic flux, because of longer constant current periods. This affected the rotary motion performance, decreased the precision and led to a higher overshoot response, resulting from the non-linear characteristics. As the rotational motion was based on the driving signal, the off-on period of the current was seen to improve the SR actuator reliability and resulted in a better open-loop response performance. In this study, the applied step input signal, with a 4s on-time period, is known as the normal signal. Here, the researchers compared 3 signal types, i.e., (i) Step input signal, (ii) Sine waveform and (iii) Pulse input signals. These signals were tested with different frequencies, wherein the on and the off-time sequences were frequently changed to allow for the discharging effect, though a single-excitation current was applied. For the pulse input signal, the duty ratio was varied with regards to the frequency, as shown in Figure 14. Table 6 describes the detailed on-time period.

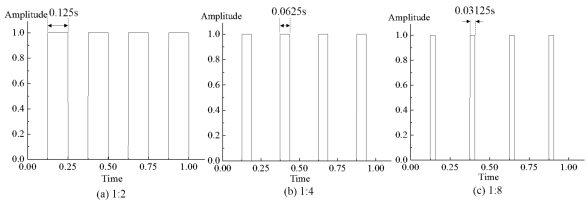

Figure 14 A 4Hz pulse input signal parameters for varying frequencies and duty ratios

Table 6 Assigned pulse input signal parameters for varying frequencies and duty ratios

Frequency	On-time of duty ratio (s)		
	1:2	1:4	1:8
1	0.5	0.25	0.125
4	0.125	0.0625	0.03125
5	0.1	0.05	0.025
6	0.0833	0.04167	0.0208
10	0.05	0.025	0.0125
20	0.025	0.0125	0.00625

Figure 14 presents the rotary motion characteristics of various driving waveform signals having a similar 0° initial position. Compared to the reference positions (indicated in the form of a square symbol), the pulse input signal, with an intermediate frequency, ranging between 4 and 6Hz, displayed an irregular response so that it exceeded the SR actuator working range, which showed a rotary angle >120°. The researchers stated that the resulting rotary motion was more stable compared to other frequencies. Hence, this frequency is prevented in actual applications, since it showed an unpredictable motion.

The sine waveforms were incompatible for all frequencies that produced a higher position error, between 8° and 12°. This was higher than the acceptable 5% position error or 3°, which was an acceptable single-excitation value [14]. Hence, this signal must not be included. These characteristics of an SR actuator indicated that it was a digital actuator, which was dependent on the fixed step signals. These unstable rotary motion characteristics for a sine waveform occurred because of the extreme changes in the polarity, for the specific sine waveform signal. This led to chaotic magnetic flux directions within the core that were not synchronized with all rotary motions.

Since the SR actuator can be applied to the fixed step signal, the pulse input signal with a 1:2 and 1:4 duty ratio showed the best performance. However, owing to the instability of the pulse input signals using a 1:2 duty ratio at the intermediate frequency, the researchers considered the 1:4 duty ratio as it delivered a better position error for all frequencies. A 20Hz frequency showed the best performance amongst all the applied frequencies, with an improved normal applied step input signal characteristic, as described in Table 7. However, this signal configuration showed a 9.26% and 12.3% higher value of %OS and Ts respectively. Despite these values, the characteristic was still with the acceptable values of %OS for the single step motion. The standard deviation showed a higher improvement, σ=0.176 with an 82.40% reduction compared to the step input signals, which showed a better precision in every repetition. Additionally, it showed a better accuracy, with a steady-state error, ess=1.175°, which decreased by 31.88%. This value was within the acceptable ±3°, which was known as the general stepper motor accuracy specification. Furthermore, the nonlinear SR actuator characteristics were based on the driving signal. Despite its limitations, this improved model can be further developed for increasing the multi-excitation current, after adopting better signal configurations mentioned in this study.

Table 7 A comparison of the performances of the rotary motion responses

Characteristic	Magnitudes	
	Step input	20Hz, 1:4 Pulse input signal
Percentage Overshoot, %OS	65.98	72.09
Settling time, Ts (s)	1.412	1.586
Standard Deviation, σ (°)	1.000	0.176
Steady-state error, ess (°)	1.725	1.175

6.0 CONCLUSION

The SR actuator was seen to be electromagnetic, incremental drive actuator, which displayed several advantages like a low construction cost, owing to its basic mechanical design, lack of a permanent magnet, rugged structure and a faster response, without any induction. Earlier studies focused on developing an SR actuator for motoring applications, which did not consider motion performances like accuracy and precision. Hence, in this study, the researchers investigated the ability of an SR actuator to operate in the precision motion systems, along with classical PID controllers. However, the SR actuator showed highly nonlinear characteristics. For using the SR actuator in other control systems, the system needs to be characterized further, using a look-up table, also known as the linearizer unit. Therefore, the researchers have characterized the system in this study with regards to their rotary motion properties like varying initial positions and the excitation current value. They observed that despite these characterizations, the performance of a normal step input signal showed a higher discharging effect, which affected its motion performance. The researchers identified an appropriate driving signal in this study, i.e., a pulse input signal of 20Hz and a 1:4 duty ratio configuration, which significantly improved its accuracy and precision. This study primarily investigated the general SR actuator characteristics to enable its application in the precision motion systems. The researchers have also described the structure and materials to be used in an SR actuator, thereby describing the characterization techniques that must be investigated further.

Acknowledgement

The authors are gratefulness to Motion Control Research Laboratory (MCon Lab), Center for Robotics and Industrial Automation (CeRIA) and Universiti Teknikal Malaysia Melaka (UTeM) for supporting the research and publication. This research is funded by Ministry of Education Malaysia (MOE) under the Fundamental Research Grant Scheme (FRGS) grant no. FRGS/2018/FKE-CERIA/F00353.

References

[1] Teodorescu, S., Vandenplas, S., Depraetere, B., Anthonis, J., Steinhauser, A., and Swevers, J. 2016. A Fast Pick-and-place Prototype Robot: Design and Control. *IEEE Conference on Control Applications (CCA), Sep. 2016*. 1414-1420.

[2] Giouroudi, I. 2008. Development of a Microgripping System for Handling of Microcomponents. *Precision Engineering*. 32: 148-152.

[3] Desai, P. C., Krishnamurthy, M., Schofield, N., and Emadi, A. 2009. Switched Reluctance Machines with Higher Rotor Poles than Stator Poles for Improved Output Torque Characteristics. *35th Annual Conference of IEEE Industrial Electronics, Nov. 2009*. 1338-1343.

[4] Pan, J., Cheung, N. C., and Yang, J. 2005. High-precision Position control of a Novel Planar Switched Reluctance Motor. *IEEE Trans. Ind. Electron*. 52(6): 1644-1652.

[5] Hyeonwoo, K., Hyoryong, L., Hyunchul, C., and Sukho, P. 2020. Analysis of Drivable Area and Magnetic Force in Quadrupole Electromagnetic Actuation System with Movable Cores. *Measurement*. 161: 1-12.

[6] Wang, S., Sato, K., and Kagawa, T. 2014. Precise Positioning of Pneumatic Artificial Muscle Systems. *Journal of Flow Control, Measurement & Visualization*. 2: 138-153.

[7] Ghazaly, M. M., and Sato, K. 2013. Characteristic Switching of a Multilayer Thin Electrostatic Actuator by a Driving Signal for an Ultra-precision Motion Stage. *Precision Engineering*. 37(1): 107-116.

[8] Wang, S., and Sato, K. 2016. High-precision Motion Control of a Stage with Pneumatic Artificial Muscles. *Precision Engineering*. 43: 448-461.

[9] Nazmin, M., Kokumai, H., and Sato, K. 2017. Development and Precise Positioning Control of a Thin and Compact Linear Switched Reluctance Motor. *Precision Engineering*. 48: 265-278.

[10] Yan, Q., Wenbo, D., and Liping, Z. 2020. Fractionated Payload 3-DOF Attitude Control using only Electromagnetic Actuation. *Aerospace Science and Technology*. 107: 1-16.

[11] Jiayu, L., and Siqin, C. 2019. Precise Motion Control of an Electromagnetic Valve Actuator with Adaptive Robust Compensation of Combustion Force. *Journal of the Franklin Institute*. 356(4): 1750-1770.

[12] Chi, Z., and Xu, Q. 2015. Precision Control of Piezoelectric Actuator using Fuzzy Feedback Control with Inverse Hysteresis Compensation. *IEEE International Conference on Nano/Micro Engineered and Molecular Systems, April 2015*. 219-224.

[13] George, T. C. C., Fraser, C. J., Bansevicius, R. T., Habil Ramutis Tolocka, Massimo, S., Stefano, P., and Sergey, E. L. 2007. *Actuators*. CRC Press.

[14] Ionic, I., Modreanu, M., Morega, A., Ieee, M., and Boboc, C. 2017. Design and Modeling of a Hybrid Stepper Motor. *10th International Symposium on Advanced Topics in Electrical Engineering, March 2017*. 192-195.

[15] Xuerong, L., Jingmeng, L., Weihai, C., and Shaoping, B. 2020. Analytical Magnetics and Torque Modeling of a Multi-layer Electromagnetic Driven Spherical Motion Generator. *Journal of Magnetism and Magnetic Materials*. 493: 1-11.

[16] Taufer, T., Billet, L., Moving, M. M. T., and Technologies, M. 2015. Compact BLDC & Stepper Motor Technology for Ultra-Slim Actuators. *Symposium Innovative Small Drives, Sept. 2015*. 24-29.

[17] Han, W. N., Liu, L. W., and Yu, P. 2014. Application of Stepping Motor in Cutting Fixed-scale Sheets. *Control Engineering and Information Systems*. CRC Press. 41-45.

[18] Widmer, J. D., Martin, R., and Kimiabeigi, M. 2015. Sustainable Materials and Technologies Electric Vehicle Traction Motors without Rare Earth Magnets. *Sustain. Mater. Technol.* 3: 7-13.

[19] Raminosoa, T., El-refaie, A., Torrey, D., Grace, K., Pan, D., Grubic, S., and Bodla, K. 2016. Test Results for a High Temperature Non-permanent Magnet Traction Motor. *IEEE Trans. Appl.* 53(4): 3496-3504.

[20] Srivastava, K., Singh, B. K., Arya, K. V., and Singh, R. K. 2011. Simulation and Modeling of 8/6 Switched Reluctance Motor using Digital Controller. *Int. J. Electron. Eng*. 3(2): 241-246.
[21] De Silva, C. W. 2015. *Sensors and Actuators*. CRC Press,
[22] Gieras, J. F. 2010. *Stepping Motors.* CRC Press.
[23] Boldea, I., Tutelea, L. N., Parsa, L., Dorrell, D., and Storage, A. E. 2014. With Reduced or No Permanent Magnets: An Overview. *IEEE Trans. Ind. Electron*. 61(10): 5696-5711.
[24] Nakazawa, Y., Ohyama, K., Nouzuka, K., Fujii, H., Uehara, H., and Hyakutake, Y. 2016. Design Method for Improving Motor Efficiency of Switched Reluctance Motor. *IEEJ Trans. Ind. Appl.*134(7): 656-666.
[25] Rahman, K. M., Fahimi, B., Suresh, G., Rajarathnam, A. V., and Ehsani, M. 2000. Advantages of Switched Reluctance Motor Applications to EV and HEV: Design and Control Issues. *IEEE Trans. Ind. Appl.* 36(1): 111-121.
[26] Xue, X. D., Cheng, K. W. E., Ng, T. W., and Cheung, N. C. 2010. Multi-objective Optimization Design of In-wheel Switched Reluctance Motors In Electric Vehicles. *IEEE Trans. Ind. Electron*. 57(9): 2980-2987.
[27] Roux, C., and Morcos, M. M. 2000. A Simple Model for Switched Reluctance Motors. *IEEE Power Eng. Rev. October*. 20: 49-52.
[28] Amorós, J. G., Blanqué Molina, B., and Andrada, P. 2013. Modelling and Simulation of a Linear Switched Reluctance Force Actuator. *IET Electr. Power Appl.* 7(5): 350-359.
[29] Chan, K. K. C., and Cheung, N. C. 2005. Characterization of a Novel Two-finger Variable Reluctance Gripper. *ISA Trans*. 44(2): 177-185.
[30] Votrubec, R., and Vavroušek, M. Control System of a Rotary Pneumatic Motor. 2014. *Proceedings of the 16th International Conference on Mechatronics – Mechatronika, Dec. 2014*. 588-593.
[31] Vavroušek, M. 2014. Identification of Pneumatic Rotational Motor. *2014 15th International Carpathian Control Conference (ICCC), May 2014*. 652-655.
[32] Ghazaly, M. M., and Sato, K. 2012. Basic Characteristics of a Multilayer Thin Electrostatic Actuator Supported by Lubricating Oil for a Fine-motion Stage. *Precis. Eng*. 36(1): 77-83.
[33] Yusri, I., Ghazaly, M. M., Ali, E. A., Alandoli, M. F., Rahmat, Z., Abdullah, M. A., Ali, M., and Ranom, R. 2016. Optimization of the Force Characteristic of Rotary Motion Type of Electromagnetic Actuator based on Finite Element Analysis. *J. Teknol*. 9(1): 13-20.
[34] Yusri, I., Ghazaly, M. M., Rahmat, M. F., Chong, S. H, Ranom, R., Abdullah, Z., Tee, S. P., and Yeo, C. K. 2016. Effects of Varying Arc Angles and Poles Numbers on Force Characteristics of Switched Reluctance (SR) Actuator. *Int. J. Mech. Mechatronics Eng. IJMME-IJENS*. 16(5): 41-47.
[35] Bilgin, B., Emadi, A., and Krishnamurthy, M. 2012. Design Considerations for Switched Reluctance Machines with a Higher Number of Rotor poles. *IEEE Trans. Ind. Electron*. 59(10): 3745-3756.
[36] Alrifai, M., Zribi, M., Rayan, M., and Krishnan, R. 2010. Speed Control of Switched Reluctance Motors Taking into Account Mutual Inductances and Magnetic Saturation Effects. *Energy Convers. Manag*. 51(6): 1287-1297.
[37] Timing, R. 2005. Engineering Dynamics. *Mechanical Engineer's Pocket Book*. Third. 87-122.
[38] Bilgin, B., Emadi, S., and Krishnamurthy, M. 2013. Comprehensive Evaluation of the Dynamic Performance of a 6/10 SRM for Traction Application in PHEVs. *IEEE Trans. Ind. Electron*. 60(7): 2564-2575.
[39] Ever, E. Hybrid Stepper Motor. 2016. [Online]. Available: *http://www.everelettronica.com/en/*. [Accessed: 20-Jun-2017].